ISSN 1392–1320 MATERIALS SCIENCE (MEDŽIAGOTYRA). Vol. 17, No. 3. 2011

Sol-Gel Synthesis and Characterization of Selected Transition Metal Nano-Ferrites

Aurelija GATELYTĖ, Darius JASAITIS, Aldona BEGANSKIENĖ, Aivaras KAREIVA *

Department of General and Inorganic Chemistry, Vilnius University, Naugarduko 24, LT-03225 Vilnius, Lithuania

http://dx.doi.org/10.5755/j01.ms.17.3.598

Received 25 October 2010; accepted 22 April 2011

In the present work, the sinterability and formation of nanosized yttrium iron garnet ($Y_3Fe_5O_{12}$), yttrium perovskite ferrite ($YFeO_3$), cobalt, nickel and zinc iron spinel ($CoFe_2O_4$, $NiFe_2O_4$ and $ZnFe_2O_4$, respectively) powders by an aqueous sol-gel processes are investigated. The metal ions, generated by dissolving starting materials of transition metals in the diluted acetic acid were complexed by 1,2-ethanediol to obtain the precursors for the transition metal ferrite ceramics. The phase purity of synthesized nano-compounds was characterized by infrared spectroscopy (IR) and powder X-ray diffraction analysis (XRD). The microstructural evolution and morphological features of obtained transition metal ferrites were studied by scanning electron microscopy (SEM).

Keywords: sol-gel, transition metals, ferrites, nanoparticles.

1. INTRODUCTION

Iron-containing transition metal oxide phases have been the subject of extensive investigations. These oxides possess unique magnetic, magneto-optical, magnetoresistive, thermal, electric and mechanical properties such as ferrimagnetizm, excellent creep and radiation damage resistance, high thermal conductivity, high electrical resistivity, controllable saturation magnetization, moderate thermal expansion coefficients, energy-transfer efficiency, narrow linewidth in ferromagnetic resonance and others [1 – 9]. These properties make iron-containing oxides suitable for numerous device applications, including magnetic materials (circulators, oscillators, phase shifters for microwave region), sensors, magneto-optic sensors, anode materials for batteries, catalysts, sensors in space applications, lasers, phosphorescent sources, microwave and electrochemical devices, black and brown pigments. Since these magneto-particles have also been shown to be non-cytotoxic, they would be suitable for biotechnological applications.

Nanostructured iron-containing transition metal oxide materials are known to exhibit interesting physical and chemical properties, significantly different from those of conventional bulk materials, due to their extremely small size and large specific surface area. Among these nanostructured materials of different shapes and sizes, transition metal ferrite nanoparticles have found considerable interest due to their technological promising applications in the microwave industries, in fields as magnetic storage, for high speed digital tape or disk recording, the production of repulsive suspensions for use in levitated railway systems, for bioassay application and application in biomedicine, ferrofluids, catalysts and magnetic refrigeration systems [10 – 18].

The preparation and characterization of nanosized structures have attracted increasing attention to researchers and scientists in the last decade. Moreover, all mentioned properties of iron-containing oxide ceramics are highly sensitive not only to the changes in dopant composition or host stoichiometry, but also to the processing conditions, which are very much responsible for the crystallinity, crystal shape, crystal size, crystal size distribution and phase purity of the resulting powders. In order to prepare these iron-containing mixed oxides, the oxide-mixing method based on the solid state reaction between the component metal oxides is still utilized because of its lower manufacturing cost and simpler preparation process [19]. However, this method, in general, requires the calcination temperature higher than 1000 °C to eliminate the unreacted starting oxides and to obtain the final product of a single phase. In order to overcome these inevitable disadvantages arising from the solid state reaction, some methods including sol-gel [20], hydrothermal [21], combustion [22], auto-combustion [23], polymeric precursor route [24], solvothermal [25] and coprecipitation [26] techniques can be used.

Over the last few decades, the sol-gel techniques have been used to prepare a variety of mixed-metal oxides, nanomaterials and nanoscale architectures, nanoporous oxides, organic-inorganic hybrids [27 – 31]. It has been demonstrated that the sol-gel process offers considerable advantages such as better mixing of the starting materials and excellent chemical homogeneity in the final product. Moreover, the molecular level mixing and the tendency of partially hydrolyzed species to form extended networks facilitate the structure evolution thereby lowering the crystallization temperature. Recently for the preparation of different garnets, aluminates, cobaltates and superconductors we elaborated an aqueous glycolate sol-gel processing route [29, 31 – 34]. In this paper we present results of a systematic study of modified aqueous sol-gel synthetic approach to pure nanosized selected transition metal ferrites (yttrium iron garnet ($Y_3Fe_5O_{12}$), yttrium perovskite ferrite ($YFeO_3$), cobalt, nickel and zinc iron spinel ($CoFe_2O_4$, $NiFe_2O_4$ and $ZnFe_2O_4$, respectively) powders). The results are presented herein.

*Corresponding author. tel.: +370-5-2193110; fax: +370-5-2330987.
E-mail address: *aivaras.kareiva@chf.vu.lt* (A. Kareiva)

2. EXPERIMENTAL

All transition metal ferrite ceramic samples ($YFeO_3$, $Y_3Fe_5O_{12}$, $CoFe_2O_4$, $NiFe_2O_4$, $ZnFe_2O_4$) were synthesized by an aqueous glycolate sol-gel method. The gels were prepared using stoichiometric amounts of analytical-grade iron nitrate nonahidrate $Fe(NO_3)_3 \cdot 9H_2O$, yttrium oxide Y_2O_3, cobalt acetate tetrahydrate $Co(CH_3COO)_2 \cdot 4H_2O$, nickel acetate tetrahydrate $Ni(CH_3COO)_2 \cdot 4H_2O$, and zinc acetate dihydrate $Zn(CH_3COO)_2 \cdot 2H_2O$, as Fe^{3+}, Y^{3+}, Co^{2+}, Ni^{2+} and Zn^{2+} raw materials, respectively. For the preparation of all samples by the sol-gel process, iron nitrate was first dissolved in 50 mL of 0.2 mol/L CH_3COOH at 65 °C. To this solution, yttrium oxide dissolved in acetic acid, or cobalt acetate, or nickel acetate, or zinc acetate dissolved in 50 mL of distilled water was added and the resulting mixture was stirred for 1 h at the same temperature. In a following step, 1,2-ethanediol (2 mL) as complexing agent was added to the reaction solution. After concentrating the solutions by a rapid evaporation at 95 °C under stirring, the Y-Fe-O, Co-Fe-O, Ni-Fe-O or Zn-Fe-O nitrate-acetate-glycolate sols turned into brownish transparent gels. The oven dried (110 °C) precursor gel powders were ground in an agate mortar and preheated for 2 h at 800 °C in air. After grinding in an agate mortar, the powders were additionally sintered in air for 10 h at 1000 °C without an intermediate grinding. The flow chart of the sol-gel synthesis of transition metal ferrites is presented in Fig. 1.

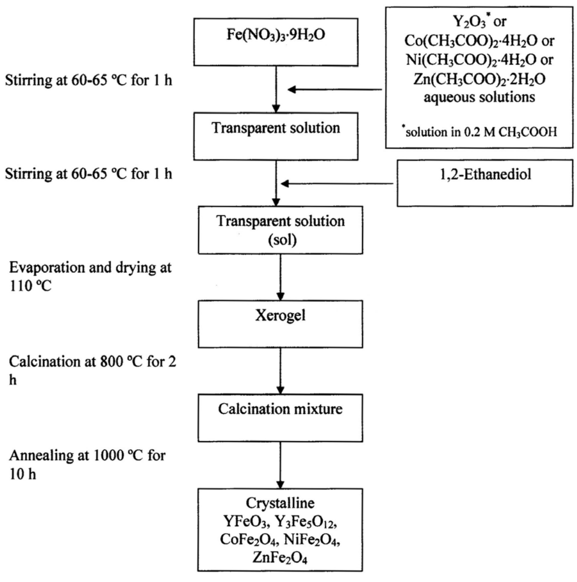

Fig. 1. Scheme of sol-gel preparation of nanosized $YFeO_3$, $Y_3Fe_5O_{12}$, $CoFe_2O_4$, $NiFe_2O_4$, and $ZnFe_2O_4$

Infrared spectra of samples in KBr pellets were recorded with a Bruker Equinox 55/S/NIR FTIR spectrometer (resolution 1 cm^{-1}). X-ray diffraction analysis (XRD) was performed on a Bruker AXE D8 Focus diffractometer with a LynxEye detector using Cu K_{α} radiation. The particle size and morphology of the resultant transition metal ferrite powders were examined using FE-SEM Zeiss Ultra 55 field emission scanning electron microscope with In-Lens detector.

3. RESULTS AND DISCUSSIONS

IR spectroscopy was used as additional tool for the structural characterization of the ceramic materials obtained by the aqueous sol-gel method. The IR spectra of ceramic materials obtained after the calcinations of the Y-Fe-O gels having different molar ratio of metals Y : Fe = 1 : 1 and Y : Fe = 3 : 5 are shown in Figs. 2 and 3, respectively.

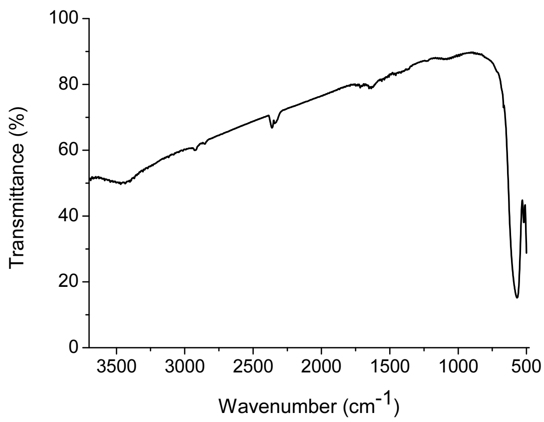

Fig. 2. Infrared spectrum of $YFeO_3$

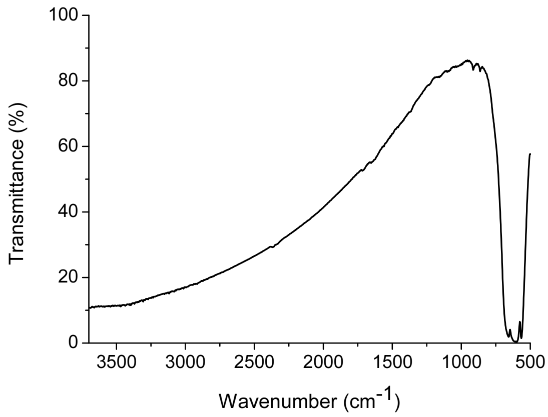

Fig. 3. Infrared spectrum of $Y_3Fe_5O_{12}$

The IR spectrum of synthesized $YFeO_3$ ceramics show broad absorption bands arising from O–H stretching and bending vibration of water due to the exposure of the sample to the atmosphere at ~3500 cm^{-1} and ~1600 cm^{-1}, respectively. Weak band at *ca.* 2350 cm^{-1} presented in spectrum belongs to carbon dioxide from atmosphere. This band appears in many spectra due to inequalities in path length. Importantly, in the 1300 cm^{-1} – 400 cm^{-1} fingerprint region, one sharp band was present at around 564 cm^{-1} is typical metal-oxygen absorption for the perovskite-type compounds. Evidently, the character of this region of IR spectrum for Y : Fe = 3 : 5 sample (see Fig. 3) is a little different. The most important feature is that several intensive bands are determined in the region of 900 cm^{-1} – 450 cm^{-1}, which may be attributed to the stretching modes of the isolated [AlO_4] tetrahedra and [AlO_6] octahedra in the garnet structure, i. e. these bands correspond to the formation of crystalline IAG. According to the literature data [35, 36], these peaks could also correspond to the metal-oxygen vibration in the dodecahedral units of garnet structure.

Fig. 4 represents IR spectra of Co-Fe-O, Ni-Fe-O and Zn-Fe-O nitrate-acetate-glycolate gels heated at 1000 °C.

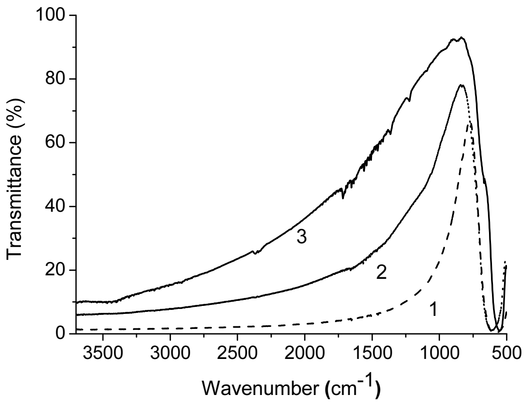

Fig. 4. Infrared spectra of $CoFe_2O_4$ (1), $NiFe_2O_4$ (2) and $ZnFe_2O_4$ (3)

As seen, all three IR spectra are almost identical with characteristic intensive absorption band located nearly 600 cm^{-1}. In preceding Fig. 4 this envelope of broad absorption is not resolved into several narrow absorption bands, as was observed for yttrium iron garnet. The observed peaks are M–O vibrations and probably are characteristic for spinel structure compounds. Consequently, the obtained IR results let us to conclude, that heat treatment of Co-Fe-O, Ni-Fe-O and Zn-Fe-O precursor gels produces corresponding spinels.

The XRD results are consistent with crystallization process observed by IR measurements. The XRD patterns of $YFeO_3$ ceramics heated at 1000 °C for 10 h is shown in Fig. 5.

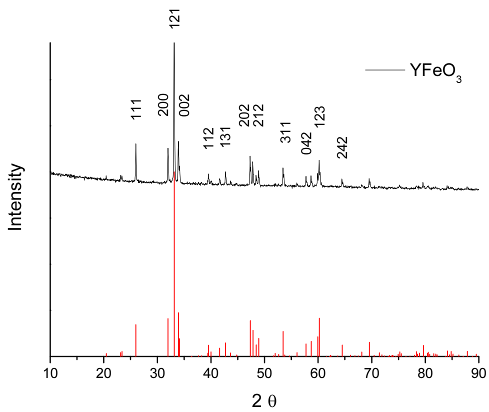

Fig. 5. X-ray diffraction pattern of $YFeO_3$ ceramics synthesized using sol-gel method at 1000 °C. Annealing time was 10 h. The Miller indices of $YFeO_3$ phase are marked

According to the XRD analysis, a fully crystallized single-phase oxide $YFeO_3$ with well pronounced perovskite crystal structure has formed (PDF No. 39-1489). No any impurity phases in the sample have been detected. The most intensive lines (121), (002) and (123) are observed at $2\theta \approx 33.1$ (100 %), 33.9 (31 %) and 60.2 (27 %), respectively. The monophasic yttrium iron garnet has also formed during heating the Y-Fe-O (Y : Fe = 3 : 5) precursor gel at 1000 °C (see Fig. 6).

The XRD pattern completely corresponds to the reference data (PDF No. 43-507). For the synthesized $Y_3Fe_5O_{12}$ the most intensive lines (420), (642) and (422) are observed at $2\theta \approx 32.3$ (100 %), 55.5 (48 %) and 35.5 (46 %), respectively.

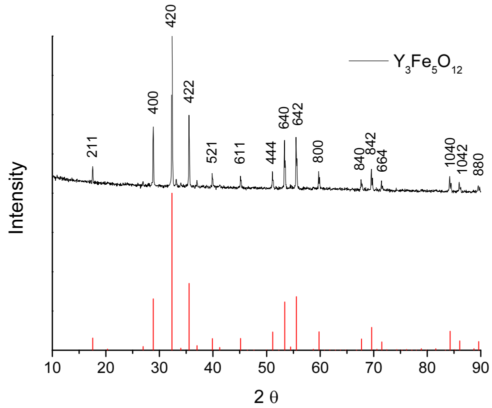

Fig. 6. X-ray diffraction pattern of $Y_3Fe_5O_{12}$ ceramics synthesized using sol-gel method at 1000 °C. Annealing time was 10 h. The Miller indices of $Y_3Fe_5O_{12}$ phase are marked

The XRD patterns of the spinel structure compounds heated at the same temperatures for 10 h are shown in Figs. 7 – 9. Surprisingly, all the samples obtained after heating of Co-Fe-O, Ni-Fe-O and Zn-Fe-O precursor gels at 1000 °C are monophasic materials. No even traces of impurity phases in the samples can be determined. The XRD data (see Fig. 7) clearly confirm the crystalline spinel structure of cobalt ferrite ($CoFe_2O_4$) to be the main crystalline component (PDF No. 22-1086). For the sol-gel derived $CoFe_2O_4$ the most intensive lines (311), (440) and (220) are observed at $2\theta \approx 35.5$ (100 %), 62.7 (41 %) and 30.2 (32 %), respectively.

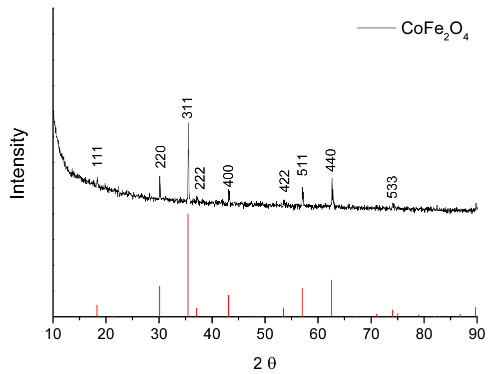

Fig. 7. X-ray diffraction pattern of $CoFe_2O_4$ ceramics synthesized using sol-gel method at 1000 °C. Annealing time was 10 h. The Miller indices of $CoFe_2O_4$ phase are marked

The XRD pattern of $NiFe_2O_4$ sample heated for 10 h is shown in Fig. 8. As seen, with substituting cobalt for nickel the obtained X-ray diffraction results consist very well with reference data (PDF No. 10-325). For the spinel structure nickel ferrite $NiFe_2O_4$ the most intensive lines (311), (220) and (440) are observed at $2\theta \approx 35.8$ (100 %), 30.3 (42 %) and 63.0 (37 %), respectively. Again, the formation of impurity phases does not proceed.

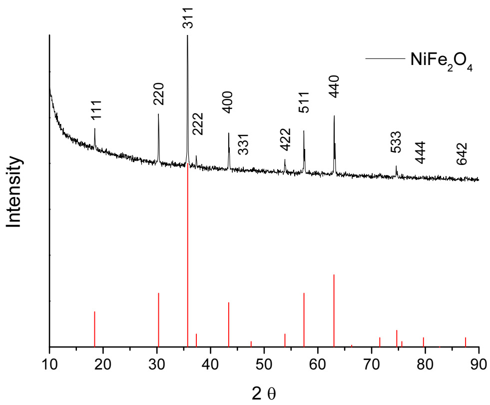

Fig. 8. X-ray diffraction pattern of $NiFe_2O_4$ ceramics synthesized using sol-gel method at 1000 °C. Annealing time was 10 h. The Miller indices of $NiFe_2O_4$ phase are marked

Fully crystalline single-phase oxide $ZnFe_2O_4$ with well pronounced spinel crystal structure have also formed at 1000 °C using the same sol-gel technique (PDF No. 22-1012). As seen from Fig. 9, for the zinc ferrite $ZnFe_2O_4$ the most intensive lines (311), (220) and (440) are observed at $2\theta \approx 35.4$ (100 %), 29.8 (39 %) and 62.3 (34 %), respectively.

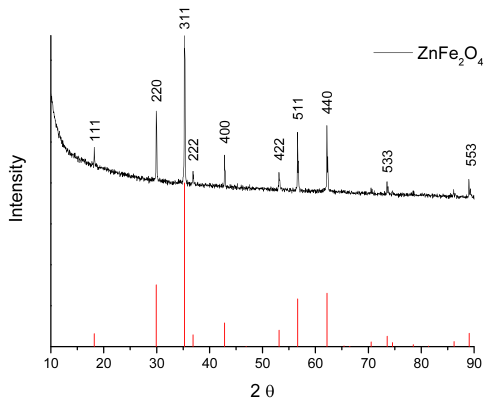

Fig. 9. X-ray diffraction pattern of $ZnFe_2O_4$ ceramics synthesized using sol-gel method at 1000 °C. Annealing time was 10 h. The Miller indices of $ZnFe_2O_4$ phase are marked

The most interesting fact is that the same synthesis conditions and the same sol-gel synthetic parameters were suitable for the preparation of monophasic different structure compounds: perovskite $YFeO_3$, garnet $Y_3Fe_5O_{12}$ and spinels $CoFe_2O_4$, $NiFe_2O_4$ and $ZnFe_2O_4$. This observation let us to conclude that the proposed simple sol-gel chemistry approach could be used for the preparation of variety crystal structure compounds.

Fig. 10 shows the SEM micrograph of $YFeO_3$ ceramics. Evidently, the scanning electron micrograph indicates the formation of nanosized crystallites of ~200 nm in width and ~1000 nm in length. The crystallites are necked to each other forming highly symmetric ornaments. Scanning electron micrograph of sol-gel derived $Y_3Fe_5O_{12}$ ceramics synthesized for 10 h at 1000 °C is shown in Fig. 11. For yttrium aluminium garnet the similar microstructure was observed as well. The same necked to each other crystallites having approximately the same size was formed. However, the particles of $Y_3Fe_5O_{12}$ formed with very well pronounced agglomeration, indicating a good connectivity between the grains.

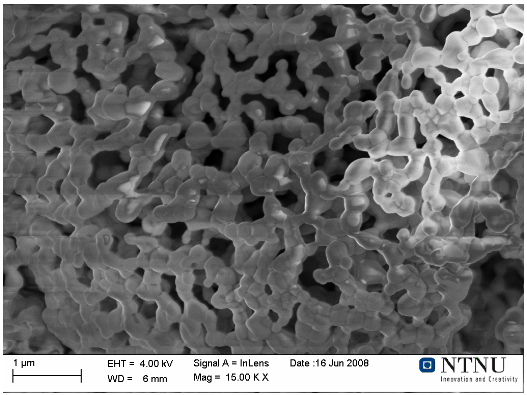

Fig. 10. Scanning electron micrograph of sol-gel derived $YFeO_3$ ceramics heated for 10 h at 1000 °C. Magnification 15000×

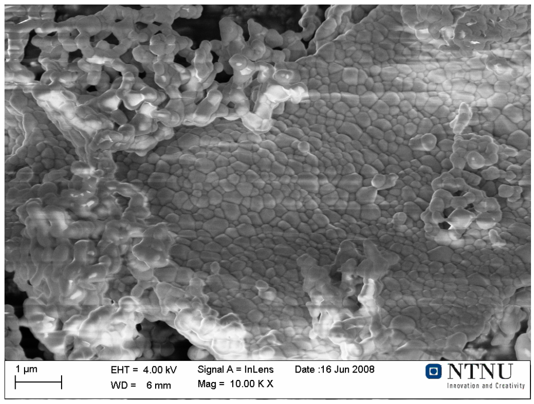

Fig. 11. Scanning electron micrograph of sol-gel derived $Y_3Fe_5O_{12}$ ceramics heated for 10 h at 1000 °C. Magnification 10000×

It is interesting to note that almost identical surface microstructure was observed for all spinel crystal structure ceramic samples. Fig. 12 shows the SEM micrograph of $CoFe_2O_4$ spinel obtained at 1000 °C.

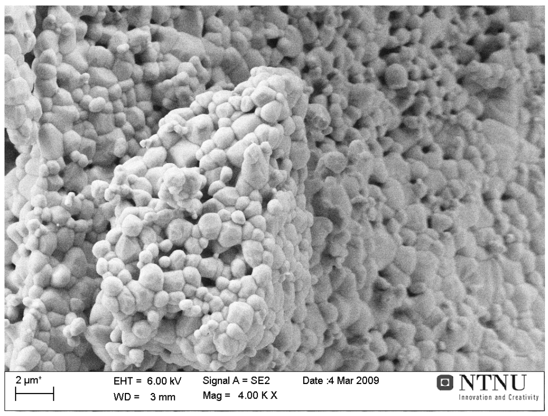

Fig. 12. Scanning electron micrograph of sol-gel derived $CoFe_2O_4$ ceramics heated for 10 h at 1000 °C. Magnification 4000×

The SEM micrograph suggests that the $CoFe_2O_4$ solids synthesized by sol-gel route are composed of spherical submicron grains (less than 1000 nm). The spherical particles are formed also in the case of nickel ferrite $NiFe_2O_4$ (see Fig. 13).

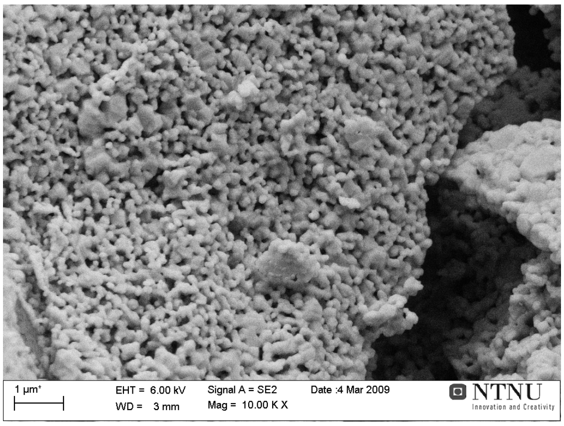

Fig. 13. Scanning electron micrograph of sol-gel derived $NiFe_2O_4$ ceramics heated for 10 h at 1000 °C. Magnification 10000×

However it seems that particle size of spinel ferrites are dependent on the nature of transition metal. $NiFe_2O_4$ crystallites mostly composed of nanoparticles with size between 100 nm and 150 nm. SEM micrograph of $ZnFe_2O_4$ ceramics is presented in Fig. 14. Zinc iron spinel ceramics was formed with an average grain size of less than 500 nm and more than 200 nm. Thus, once again we can conclude that the particle size of spinels depends on the nature of transition metal ($CoFe_2O_4 > ZnFe_2O_4 > NiFe_2O_4$). Moreover, all three spinels have formed with mesoporous structure.

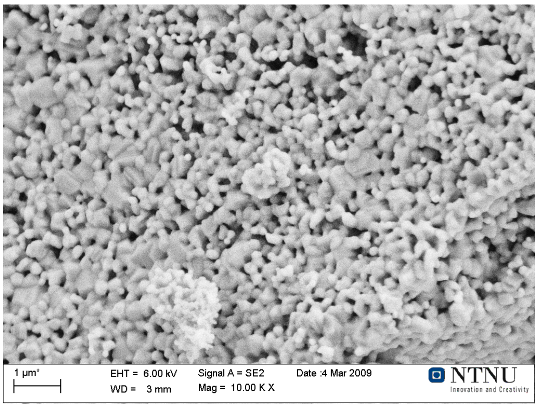

Fig. 14. Scanning electron micrograph of sol-gel derived $ZnFe_2O_4$ ceramics heated for 10 h at 1000 °C. Magnification 10000×

4. CONCLUSIONS

In this work for the synthesis of yttrium perovskite ferrite ($YFeO_3$), yttrium iron garnet ($Y_3Fe_5O_{12}$), cobalt, nickel and zinc iron spinels ($CoFe_2O_4$, $NiFe_2O_4$ and $ZnFe_2O_4$, respectively) environmentally benign an aqueous sol-gel process has been suggested. The present study demonstrates the versatility of the solution method to yield a monophasic transition metal ferrites at low sintering temperature (up to 1000 °C) when compared to the temperature required for the solid-state synthesis (>1400 °C – 1600 °C). It was demonstrated that IR spectroscopy is indispensable tool for the characterization of perovskites, garnets and spinels in the region of 900 cm^{-1} – 450 cm^{-1}. The most interesting fact is that monophasic different structure compounds (perovskite $YFeO_3$, garnet $Y_3Fe_5O_{12}$ and spinels $CoFe_2O_4$, $NiFe_2O_4$ and $ZnFe_2O_4$) have been successfully obtained by this method using the same synthetic parameters. To the best our knowledge, the nanosized transition metal ferrites were prepared by a soft sol-gel chemistry approach for the first time. Besides, the particle size of spinel ferrites is dependent on the nature of transition metal. Finally, the proposed sol-gel method of preparation of transition metal ferrites in aqueous media is inexpensive and thus appropriate for the large scale production of such type ceramics.

REFERENCES

1. **Wang, X. Y., Yang, G. Q., Zhang, Z. S., Yan, L. M., Meng, J. H.** Synthesis of Strong-magnetic Nanosized Black Pigment $Zn_xFe_{3-x}O_4$ *Dyes and Pigments* 74 2007: pp. 269 – 272.
2. **Costa, A. C. F. M., Leite, A. M. D., Ferreira, H. S., Kiminami, R. H. G. A., Cava, S., Gama, L.** Brown Pigment of the Nanopowder Spinel Ferrite Prepared by Combustion Reaction *Journal of the European Ceramic Society* 28 2008: pp. 2033 – 2037.
3. **Hossain, A. K. M. A., Biswas, T. S., Yanagida, T., Tanaka, H., Tabata, H., Kawai, T.** Investigation of Structural and Magnetic Properties of Polycrystalline $Ni_{0.50}Zn_{0.50-x}Mg_xFe_2O_4$ Materials Chemistry and Physics 120 2010: pp. 461 – 467.
4. **Naoe, M., Omura, T., Sato, T., Yamasawa, K., Miura, Y.** Synthesis and Characterization of Temperature Sensitive L-Zn-Cu Ferrite *Japanese Journal of Applied Physics* 47 2008: pp. 550 – 553.
5. **Lebourgeois, R., Coillot, C.** Mn-Zn Ferrites for Magnetic Sensor in Space Applications *Journal of Applied Physics* 103 2008: pp. Ar. # 07E510.
6. **Kim, D. H., Zeng, H. D., Ng, T. C., Brazel, C. S.** T-1 and T-2 Relaxivities of Succimer-coated $MFe_2^{3+}O_4$ (M = Mn^{2+}, Fe^{2+} and Co^{2+}) Inverse Spinel Ferrites for Potential Use as Phase-contrast Agents in Medical MRI *Journal of Magnetism and Magnetic Materials* 321 2009: pp. 3899 – 3904.
7. **Hemeda, D. M., Tawfik, A., Hemeda, O. M., Dewidar, S. M.** Effects of NiO Addition on the Structure and Electric Properties of $Dy_{3-x}Ni_xFe_5O_{12}$ Garnet Ferrite *Solid State Sciences* 11 2009: pp. 1350 – 1357.
8. **Zhou, S. Q., Potzger, K., Xu, Q. Y., Kuepper, K., Talut, G., Marko, D., Mucklich, A., Helm, M., Fassbender, J., Arenholz, E., Schmidt, H.** Spinel Ferrite Nanocrystals Embedded Inside ZnO: Magnetic, Electronic, and Magnetotransport Properties *Physical Review* B 80 2009: pp. Ar. # 094409.
9. **Hankare, P. P., Kamble, P. D., Maradur, S. P., Kadam, M. R., Sankpal, U. B., Patil, R. P., Nimat, R. K., Lokhande, P. D.** Ferrospinels Based on Cu and Co Prepared via Low Temperature Route as Efficient Catalysts for the Selective Oxidation of Alcohol *Journal of Alloys and Compounds* 487 2009: pp. 730 – 734.
10. **Ji, G., Tang, S., Xu, B., Gu, B., Du, Y.** Synthesis of $CoFe_2O_4$ Nanowire Arrays by Sol-Gel Template Method *Chemical Physics Letters* 379 2003: pp. 484 – 489.
11. **Khan, A., Chen, P., Boolchand, P., Smirniotis, P. G.** Modified Nano-crystalline Ferrites for High-temperature WGS Membrane Reactor Applications *Journal of Catalysis* 253 2008: pp. 91 – 104.

12. **Srivastava, M., Ojha, A. K., Chaubey, S., Materny, A.** Synthesis and Optical Characterization of Nanocrystalline $NiFe_2O_4$ Structures *Journal of Alloys and Compounds* 481 2009: pp. 515 – 519.

13. **Wang, X., Wang, L. Y., Lim, I. I. S., Bao, K., Mott, D., Park, H. Y., Luo, J., Hao, S. L., Zhong, C. J.** Synthesis, Characterization and Potential Application of MnZn Ferrite and MnZn Ferrite@Au Nanoparticles *Journal of Nanoscience and Nanotechnology* 9 2009: pp. 3005 – 3012.

14. **Mouli, K. C., Joseph, T. Ramam, K.** Synthesis and Magnetic Studies of Co-Ni-Zn Ferrite Nano Crystals *Journal of Nanoscience and Nanotechnology* 9 2009: pp. 5596 – 5599.

15. **Deraz, N. M., Shaban, S.** Optimization of Catalytic, Surface and Magnetic Properties of Nanocrystalline Manganese Ferrite *Journal of Analytical and Applied Pyrolysis* 86 2009: pp. 173 – 179.

16. **Senthil, S. M., Jayaprakash, R. V., Singh, N., Mehta, B. R., Govindaraj, G.** Synthesis and Magnetic Properties of Nanosized Cobalt Substituted Nickel Ferrites ($Ni_{1-x}Co_xFe_2O_4$) Using Egg White (Ovalbumin) by Thermal Evaporation *Journal of Nano Research* 4 2008: pp. 107 – 116.

17. **Roca, A. G., Costo, R., Rebolledo, A. F., Veintemillas-Verdaguer, S., Tartaj, P., Gonzalez-Carreno, T., Morales, M. P., Serna, C. J.** Progress in the Preparation of Magnetic Nanoparticles for Application in Biomedicine *Journal of Physics D-Applied Physics* 42 2009: pp. Ar. # 224002.

18. **Jalaly, M., Enayati, M. H., Kameli, P., Karimzadeh, F.** Effect of Composition on Structural and Magnetic Properties of Nanocrystalline Ball Milled $Ni_{1-x}Zn_xFe_2O_4$ Ferrite *Physica B-Condensed Matter* 405 2010: pp. 507 – 512.

19. **Li, D., Peng, Z. J., Cui, X. M., Wang, C. B., Ge, H. L., Fu, Z. Q., Yang, Y. Y.** Study on Sintering Systems on Ni-Zn Ferrites Doped with Al^{3+} by One-step Synthesis *Rare Metal Materials and Engineering* 38 2009: pp. 920 – 923.

20. **Lavela, P., Tirado, J. L.** $CoFe_2O_4$ and $NiFe_2O_4$ Synthesized by Sol-gel Procedures for Their Use as Anode Materials for Li Ion Batteries *Journal of Power Sources* 172 2007: pp. 379 – 387.

21. **Nalbandian, L., Delimitis, A. V., Zaspalis, T., Deliyanni, E. A., Bakoyannakis, D. N., Peleka, E. N.** Hydrothermally Prepared Nanocrystalline Mn-Zn Ferrites: Synthesis and Characterization *Microporous and Mesoporous Materials* 114 2008: pp. 465 – 473.

22. **Sertkol, M., Koseoglu, Y., Baykal, A., Kavas, H., Toprak, M. S.** Synthesis and Magnetic Characterization of $Zn_{0.7}Ni_{0.3}Fe_2O_4$ Nanoparticles via Microwave-assisted Combustion Route *Journal of Magnetism and Magnetic Materials* 322 2010: pp. 866 – 871.

23. **Barati, M. R., Ebrahimi, S. A. S., Badiei, A.** The Role of Surfactant in Synthesis of Magnetic Nanocrystalline Powder of $NiFe_2O_4$ by Sol-gel Auto-combustion Method *Journal of Non-Crystalline Solids* 354 2008: pp. 5184 – 5185.

24. **Gharagozlou, M.** Synthesis, Characterization and Influence of Calcinations Temperature on Magnetic Properties of Nanocrystalline Spinel Co-ferrite Prepared by Polymeric Precursor Method *Journal of Alloys and Compounds* 486 2009: pp. 660 – 665.

25. **Yanez-Vilar, S., Sanchez-Andujar, M., Gomez-Aguirre, C., Mira, J., Senaris-Rodriguez, M A., Castro-Garcia, S.** A Simple Solvothermal Synthesis of MFe_2O_4 (M = Mn, Co and Ni) Nanoparticles *Journal of Solid State Chemistry* 182 2009: pp. 2685 – 2690.

26. **Xia, A. L., Zhang, H. L.** Effects of Excessive Zn^{2+} Ions on Intrinsic Magnetic and Structural Properties of $Ni_{0.2}Zn_{0.6}Cu_{0.2}Fe_2O_4$ Powder Prepared by Chemical Coprecipitation Method *Current Applied Physics* 10 2010: pp. 825 – 827.

27. **Brinker, C. J., Scherer, G. W.** Sol-Gel Science: The Physics and Chemistry of Sol-Gel Processing. Academic Press, London, 1990.

28. **Cushing, B. L., Kolesnichenko, V. L., O'Connor, C. J.** Recent Advances in the Liquid-phase Syntheses of Inorganic Nanoparticles *Chemical Reviews* 104 2004: pp. 3893 – 3946.

29. **Katelnikovas, A., Barkauskas, J., Ivanauskas, F., Beganskiene, A., Kareiva, A.** Aqueous Sol-Gel Synthesis Route for the Preparation of YAG: Evaluation of Sol-Gel Process by Mathematical Regression Model *Journal of Sol-Gel Science and Technology* 41 2007: pp. 193 – 201.

30. **Mackenzie, J. D., Bescher, E. P.** Chemical Routes in the Synthesis of Nanomaterials Using the Sol-Gel Process *Accounts of Chemical Research* 40 2007: pp. 810 – 818.

31. **Baranauskas, A., Jasaitis, D., Kareiva, A.** Characterization of Sol-Gel Process in the Y-Ba-Cu-O Acetate-Tartrate System Using IR Spectroscopy *Vibrational Spectroscopy* 28 2002: pp. 263 – 275.

32. **Cizauskaite, S., Reichlova, V., Nenartaviciene, G., Beganskiene, A., Pinkas, J., Kareiva, A.** Sol-Gel Preparation and Characterization of Gadolinium Aluminate *Materials Chemistry and Physics* 102 2007: pp. 105 – 110.

33. **Katelnikovas, A., Justel, T., Uhlich, D., Jorgensen, J.-E., Sakirzanovas, S., Kareiva, A.** Characterization of Cerium-doped Yttrium Aluminium Garnet Nanopowders Synthesized via Sol-Gel Process *Chemical Engineering Communications* 195 2008: pp. 758 – 769.

34. **Klemkiene, T., Raudonis, R., Beganskiene, A., Zalga, A., Grigoraviciute, I., Kareiva, A.** Scandium and Gallium Substitution Effects in the $(Y_{1-x}Sc_x)Ba_2Cu_4O_8$ and $(Y_{1-x}Ga_x)Ba_2Cu_4O_8$ Superconducting Oxides *Materials Chemistry and Physics* 119 2010: pp. 208 – 213.

35. **Vaqueiro, P., Lopez-Quintela, M. A.** Influence of Complexing Agents and pH on Yttrium-Iron Garnet Synthesized by the Sol-Gel Method *Chemistry of Materials* 9 1997: pp. 2836 – 2841.

36. **Vaqueiro, P., Lopez-Quintela, M. A.** Synthesis of Yttrium Aluminium Garnet by the Citrate Gel Process *Journal of Materials Chemistry* 8 1998: pp. 161 – 163.